REPETITIVE IMPACT BETWEEN TWO ORTHOGONAL BEAMS

Elizabeth K. Ervin, A.M. ASCE
Civil Engineering, The University of Mississippi, University, Mississippi, 38677
eke@olemiss.edu

Abstract

Contact between two beam-like structures is a situation that occurs in piping systems, among other applications. For example, anti-vibration bars are fitted between the tubes in some steam generator designs. The interference fit can become worn and impact can take place between the tube and bar when either becomes worn. This paper investigates the repetitive impact dynamics of two orthogonal pinned-pinned beams subjected to base excitation at specified frequency and acceleration. The orthogonal beam configuration restricts the contact to a single point, and the contact interface between the beams is modeled by a spring. This analysis for the impact of two beams is an extension of previous simulations of a single beam impacting a compliant support. While many approaches have been developed for multi-body dynamics, the constraint and modal mapping method is applied herein to obtain the forced response through modal analysis. The vibration is described in a piecewise fashion as switching between the linear in-contact and not-in-contact states, and compatibility conditions are applied at their junctions. The development of the conjoined mode shapes and their orthogonality is derived in detail. The contact impulse is used to describe the repetitive impact frequency response functions and their complexity.

Introduction

Nuclear reactor components, the motivating technology behind this work, are susceptible to damage from contact due to repetitive impact. As the motivating application for this thesis, nuclear power plants are a class of structures for which impact-driven vibration is of concern. Contact can occur between reactor rods or steam generator tubes and their respective supports. Such motions are driven by fluid flow or ship-borne vibration sources. The resulting impacts and vibration not only can cause undesirable fretting and wear of such sensitive components but can also introduce contaminants into the reactor's fluids systems (Ko, 1996). While beam-like nuclear reactor components are the specific motivating application, repetitive impact affects a variety of machinery, manifesting as noise, wear, or damage. Additional examples include an oil-well drill string, which experiences axial, torsional, and lateral vibrations as well as repeated tip impacts on hard rock (Tucker and Wang, 1999); check valves, which impact upon closure in such critical locations as the human heart (Kepner and Cao, 1996); and gears sets, which are designed to minimize vibration and noise yet require surface-to-surface contact.

Many approaches have been utilized to examine multibody dynamics including finite element (Schiehlen and Seifried, 2004), impulse-momentum balance (Shabana and Gau, 1993), and wave propagation. An energy conservation method is used by Allwood and Ciftci (2005) for the tribological study of rough contact. That is, the loss of energy per impact corresponds with the deterioration of surface topography over time. Marghitu and Hurmuzlu (1996) examined multiple collisions at incidence angles that induce friction as prescribed by Coulomb's law. Specifically addressing the contact of flexible bodies, Teng

and Wierzbicki (2005) employed the wave propagation approach to investigate high velocity beam-to-beam impacts. A beam was successively impacted by orthogonal beams traveling at a constant velocity. Since the study's motivation was the World Trade Center attacks on September 11, 2001, the critical number of impacts to cause local shear failure was determined, and focus was placed on the stricken beam's transient deflection and velocity as well as tensile strain and critical impact velocity.

This paper investigates the repetitive impact dynamics of two orthogonal pinned-pinned beams subjected to base excitation at specified frequency and acceleration. Such a model is representative of contact and impact between pipes in a fluid network, for instance. The orthogonal beam configuration restricts the contact to a single point, and the contact interface between the beams is modeled by a spring. An innovative method for this analysis of impacting beam structures that can capture their rich dynamics is developed from the previous work of Ervin and Wickert (submitted). Using the constraint and modal mapping method, the forced response is obtained using modal analysis, and the contact impulse is used to describe the repetitive impact frequency response functions and their complexity.

Vibration Model

Figure 1 illustrates two orthogonal beams having pinned end conditions. Each beam $i = 1$ or 2 is rectangular in cross-section with areas A_i as the product of depth b_i and height h_i, and the second moments of area are denoted $I_i = b_i\, h_i^3 / 12$. Beams "1" and "2" likewise have flexural rigidities E_1I_1 and E_2I_2, volumetric densities ρ_1 and ρ_2, and lengths L_1 and L_2. The lateral displacement and the location of contact on beam i are denoted by $w_i\,(x_i,t)$ and x_{ic}, respectively. The contact interface is modeled by a spring of stiffness k, which has deadband clearance c. Numerical values for these parameters are listed in Table 1.

Motion of the two-beam system is viewed as switching sequentially between two states $S^{(j)}$ within which vibration is linear: State $j = 0$ refers to the configuration in which contact does not occur, and state $j = 1$ refers to the case in which contact occurs. The configuration of the system in either state is given by $w_1(x_1,t)$ and $w_2(x_2,t)$. The gap between the beams is $w_1(x_1,t) - w_2(x_2,t)$. When the gap is greater than the deadband clearance c, the beams act independently with the equations of motion

$$\rho_1 A_1 w_{1,tt}(x_1,t) + E_1 I_1 w_{1,xxxx}(x_1,t) = 0 \tag{1}$$

$$\rho_2 A_2 w_{2,tt}(x_2,t) + E_2 I_2 w_{2,xxxx}(x_2,t) = 0 \tag{2}$$

where the comma-subscript notation implies partial differentiation. The "x" subscript denotes differentiation with respect to x_1 for terms involving w_1, and with respect to x_2 for terms involving w_2.

The beams have pinned supports and base excitation $e(t)$. The boundary conditions are $w_1(0,t) = e(t)$, $w_{1,xx}(0,t) = 0$, $w_1(L_1,t) = e(t)$, $w_{1,xx}(L_1,t) = 0$, $w_2(0,t) = e(t)$, $w_{2,xx}(0,t) = 0$, $w_2(L_2,t) = e(t)$, and $w_{2,xx}(L_2,t) = 0$. With the superposition $w = v + e(t)$, the boundary

conditions on v_1 and v_2 become homogeneous, or $v_1(0,t) = 0$, $v_{1,xx}(0,t) = 0$, $v_1(L_1,t) = 0$, $v_{1,xx}(L_1,t) = 0$, $v_2(0,t) = 0$, $v_{2,xx}(0,t) = 0$, $v_2(L_2,t) = 0$, and $v_{2,xx}(L_2,t) = 0$. The equations of motion then become

$$\rho_1 A_1 v_{1,tt}(x_1,t) + E_1 I_1 v_{1,xxxx}(x_1,t) = f_1 \quad (3)$$
$$\rho_2 A_2 v_{2,tt}(x_2,t) + E_2 I_2 v_{2,xxxx}(x_2,t) = f_2 \quad (4)$$

with the body forces $f_i = -\rho_i A_i e_{,tt}$ created by superposition. For the in-contact state,

$$\rho_1 A_1 v_{1,tt}(x_1,t) + E_1 I_1 v_{1,xxxx}(x_1,t) = k(v_2(x_{2c},t) - v_1(x_{1c},t))\delta(x_1 - x_{1c}) + f_1 \quad (5)$$
$$\rho_2 A_2 v_{2,tt}(x_2,t) + E_2 I_2 v_{2,xxxx}(x_2,t) = k(v_1(x_{1c},t) - v_2(x_{2c},t))\delta(x_2 - x_{2c}) + f_2 \quad (6)$$

where δ is Dirac's delta function. If the state of the two-beam system is given by $\underline{u} = [v_1(x,t) \quad v_2(x,t)]^T$, then the motion is described by $\underline{M}\,\underline{u}_{,tt} + \underline{K}\,\underline{u} = \underline{f}$ where the inertia operator $\underline{M}$ is

$$\underline{M}^{(j)}\underline{u} = \begin{bmatrix} \rho_1 A_1 v_1(x_1,t) \\ \rho_2 A_2 v_2(x_2,t) \end{bmatrix} \quad (7)$$

and $\underline{f} = [-\rho_1 A_1 e_{,tt} \quad -\rho_2 A_2 e_{,tt}]^T$. The stiffness operator in $S^{(0)}$ is

$$\underline{K}^{(0)}\,\underline{u} = \begin{bmatrix} E_1 I_1 v_{1,xxxx}(x_1,t) \\ E_2 I_2 v_{2,xxxx}(x_2,t) \end{bmatrix} \quad (8)$$

and in $S^{(1)}$, it is given by

$$\underline{K}^{(1)}\,\underline{u} = \underline{K}^{(0)}\,\underline{u} + \begin{bmatrix} k(v_1(x_{1c},t) - v_2(x_{2c},t))\delta(x_1 - x_{1c}) \\ k(v_2(x_{2c},t) - v_1(x_{1c},t))\delta(x_2 - x_{2c}) \end{bmatrix}. \quad (9)$$

Orthogonality of the state vector with respect to the inertial and stiffness operators must be proven for both $S^{(1)}$ and $S^{(1)}$ so that modal analysis can be applied in a standard fashion. While orthogonality with respect to $\underline{M}^{(j)}$ is trivial, the self-adjoint and positive definite proofs are complex for both $\underline{K}^{(0)}$ and $\underline{K}^{(1)}$. The proofs have been completed by the author and will be published at a later date.

Free Vibration

Synchronous solutions for free vibration within each state $S^{(j)}$ are sought such that $\underline{v}^{(j)} = \underline{\phi}^{(j)} \sin(\omega t)$. The mode shapes $\underline{\phi}_m^{(j)}$ for mode m are given by $\underline{\phi}_m^{(j)} = [V_{1m}^{(j)}(x_1) \quad V_{2m}^{(j)}(x_2)]^T$ where V_1 and V_2 correspond to the shapes of beam "1" and beam "2," respectively. The characteristic equation for each state is solved for the system's natural frequencies and mode shapes. The not-in-contact mode shapes $\underline{\phi}^{(0)}$ result from the uncoupled $\underline{K}^{(0)}$ and boundary conditions, while the conjoined mode shapes $\underline{\phi}^{(1)}$ are additionally constrained by the deflection and slope compatibility conditions that are embedded in $\underline{K}^{(1)}$.

The $S^{(1)}$ natural frequencies are dependent upon the stiffness of the contact interface for two identical beams. For the uncoupled case, four repeated modes occur, consisting each of the beams' independent classical mode shapes. As k increases, the repeated modes involving the beams' symmetric displacements separate into two modes with differing natural frequencies. The repeated modes involving the beams' anti-symmetric modes remain the same since the contact occurs at a nodal point.

The motion of the beams in $S^{(j)}$ is represented as the superposition

$$\underline{u}^{(j)}(x,t) \approx \sum_{m=1}^{N} \eta_m^{(j)}(t)\, \underline{\phi}_m^{(j)}(x) \tag{10}$$

where $\eta_m^{(j)}(t)$ are generalized coordinates for the m^{th} mode of state j. Each modal coordinate satisfies the ordinary differential equation

$$\ddot{\eta}_m^{(j)} + 2\xi^{(j)}\omega_m\dot{\eta}_m^{(j)} + \omega_m^2\eta_m^{(j)} = \langle \underline{f}, \underline{\phi}_m^{(j)} \rangle \tag{11}$$

where $\xi^{(j)}$ is the modal damping ratio for the system in state j. The j^{th} modal force term is the projection of the body force vector onto the corresponding mode shape.

Mapping Between States

Switching between states occurs when there is impact between the spring segments, or loss-of-contact between the two. At those conditions, $w_1(x_{1c},t) - w_2(x_{2c},t) = c^*$ where $c^* = c + h_1/2 - h_2/2$. The roots of this equation identify the instants at which gap function passes through zero. The beams' displacements and velocities just before impact are identical to those just afterwards: these compatibility conditions between states are used to derive the state-to-state transformation matrices $\underline{T}^{(01)}$ and $\underline{T}^{(10)}$. At an impact t_k, the modal coordinates for each beam are transformed between $S^{(0)}$ and $S^{(1)}$ by

$$\begin{aligned} \underline{\eta}^{(1)}(t_k^+) &= \underline{T}^{(01)}\ \underline{\eta}^{(0)}(t_k^-) \\ \underline{\dot{\eta}}^{(1)}(t_k^+) &= \underline{T}^{(01)}\ \underline{\dot{\eta}}^{(0)}(t_k^-) \end{aligned} \tag{12}$$

Determined by the state eigenvectors for both beams, the i-j element of $\underline{T}^{(01)}$ is the mass-weighted projection of modal vectors for beam i:

$$\begin{aligned} \underline{T}_{i,j}^{(01)} &= \langle \underline{M}\underline{\phi}_j^{(0)}, \underline{\phi}_i^{(1)} \rangle \\ &= \int_0^{L_1} \rho_1 A_1 V_{1j}^{(0)}\, V_{1i}^{(1)}\, dx_1 + \int_0^{L_2} \rho_2 A_2 V_{2j}^{(0)}\, V_{2i}^{(1)}\, dx_2 \end{aligned} \tag{13}$$

The companion matrix $\underline{T}^{(10)} = \underline{T}^{(01)T}$ maps the rebound from $S^{(1)}$ to $S^{(0)}$.

Limiting Case Comparison

The results of the two-beam model are compared with the single beam-rigid body model

of Ervin and Wickert (submitted) for the purpose of method verification. Beams with the parameters listed in Table 1 contact at their central points. By creating a relative stiffness for beam "2" that represents a surface, the modulus E_2 is increased such that $\omega_1^{(0)}$ for beam "2"is 10^5 that of beam "1". This model can be compared to the single beam model using the geometric parameters of beam "1" with no rigid body ($L = L_1$, $L_m = 0$). Using $k^* = 10^3$, $\omega_1^{(1)} / \omega_1^{(0)} = 4.01$. For the simulations herein, no deadband clearance exists ($c = 0$), and the load is held at a constant acceleration for each case. Two modes included in the calculations for each state, while $\xi^{(0)} = 1\%$ and $\xi^{(1)} = 5\%$.

Time histories on the relative gap between the beams, $w_1(x_1,t) - w_2(x_2,t)$, are calculated for a range of excitation frequencies. $S^{(1)}$ motion is indicated by $w_1(x_{1c},t) - w_2(x_{2c},t) - c^* < 0$, and the contact force is used to calculated the impulse to create frequency response functions. Figure 2 shows the system's repetitive impact frequency response functions for both models. After reaching steady-state, the time histories for fifteen impacts are captured and the impulse I is calculated for each cycle. The dimensionless impulse $I^* = (I \omega_1^{(0)}) / (k_b L_1)$, where k_b is the static stiffness as found with a force applied at, and displacement measured at, the midpoint of beam "1." The major features of the frequency response diagrams are similar: the system resonance at $\omega^* = 1.60$, its harmonic at $\omega^* = 3.20$ of lower magnitude, and the period-one to period-two bifurcation at $\omega^* = 2.40$. In short, the frequencies of harmonic resonances, bifurcations, and grazing impacts accurately correspond between the single beam and two beam models.

Acknowledgements

The author acknowledges Jonathan A. Wickert, Department of Mechanical Engineering, Carnegie Mellon University, for his guidance in the completion of this work.

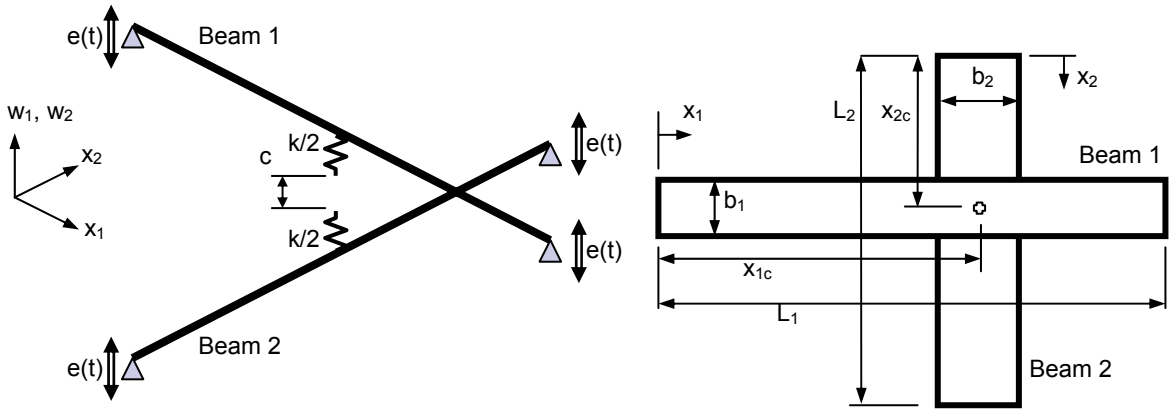

Figure 1. Two elastic beams that are subjected to base excitation and impact.

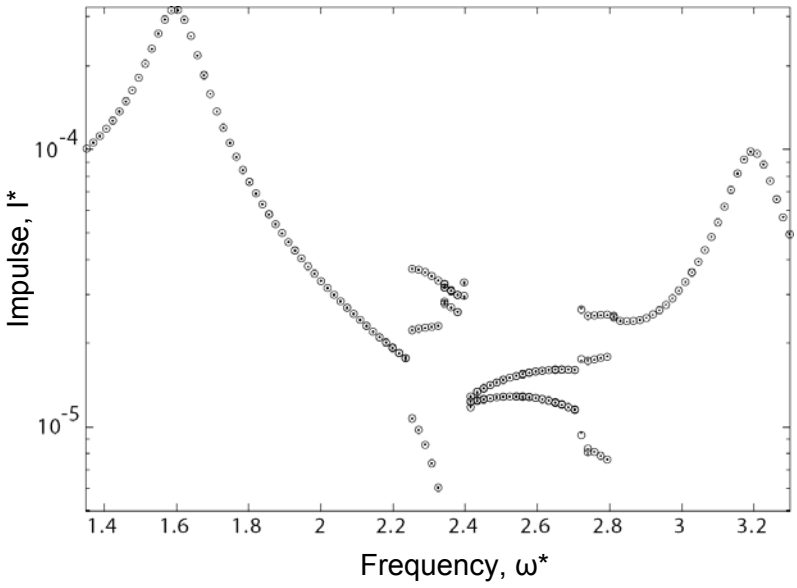

Figure 2. Repetitive impact frequency response functions for the single beam model (···) and two beam model (ooo).

Modulus of beam 1, E_1	1.66 GPa
Modulus of beam 2, E_2	166 TPa
Density, ρ_1, ρ_2	0.954 $\mathrm{Mg/m^3}$
Length, L_1, L_2	5.29 cm
Height, h_1, h_2	0.127 cm
Width, b_1, b_2	1.27 cm
Contact location on beam 1, x_{1c}	2.65 cm
Contact location on beam 2, x_{2c}	2.65 cm
Contact stiffness, k	1.78 MN/m
Clearance, c	0 cm

Table 1. Parameters for two-beam study.

References

Allwood, J., H. Ciftci (2005), "An Incremental Solution Method for Rough Contact Problems," *Wear*, **258,** 1601-1615.

Ervin, E. K., J. A. Wickert, "Repetitive Impact Response of a Beam Structure Subjected to Harmonic Base Excitation," *Journal of Sound and Vibration* (submitted).

Kepner, J., H. Cao (1996), "Effect of Repetitive Impact on the Mechanical Strength of Pyrolytic Carbon," *Journal of Heart Valve Disease*, **5,** S50-8.

Ko, P.L., M.-C. Taponat, M. Zbinden (1996), "Wear Studies of Materials for Tubes and Anti-vibration Bars in Nuclear Steam Generators," *Journal of Pressure Vessel Technology*, **118,** 287-300.

Marghitu, D. B., Y. Hurmuzlu (1996), "Nonlinear Dynamics of an Elastic Rod with Frictional Impact," *Nonlinear Dynamics*, **10,** 187-201.

Schiehlen, W. , R. Seifried (2004), "Three Approaches for Elastodynamic Contact in Multibody Systems," *Multibody System Dynamics*, **12**, 1-16.

Shabana, A. A., W. H. Gau (1993), "Propagation of Impact-induced Longitudinal Waves in Mechanical Systems with Variable Kinematic Structure," *Journal of Vibration and Acoustics*, **115**, 1-8.

Teng, X., T. Wierzbicki (2005), "Multiple Impact of Beam-to-beam," *International Journal of Impact Engineering*, **31,** 185-219.

Tucker, R. W., C. Wang (1999), "On the effective control of torsional vibrations in drilling systems," *Journal of Sound and Vibration*, **224**, 101-122.